



HAL
open science

Measurement of Correlations between Pions from Different W's in $e^+e^- \rightarrow W^+W^-$ Events

P. Abreu, W. Adam, T. Adye, I. Ajinenko, G D. Alekseev, R. Alemany, P P.
Allport, S. Almeded, S. Amato, P. Andersson, et al.

► **To cite this version:**

P. Abreu, W. Adam, T. Adye, I. Ajinenko, G D. Alekseev, et al.. Measurement of Correlations between Pions from Different W's in $e^+e^- \rightarrow W^+W^-$ Events. Physics Letters B, 1997, 401, pp.181-191. 10.1016/S0370-2693(97)00419-X . in2p3-00001132

HAL Id: in2p3-00001132

<https://hal.in2p3.fr/in2p3-00001132>

Submitted on 17 Nov 1998

HAL is a multi-disciplinary open access archive for the deposit and dissemination of scientific research documents, whether they are published or not. The documents may come from teaching and research institutions in France or abroad, or from public or private research centers.

L'archive ouverte pluridisciplinaire **HAL**, est destinée au dépôt et à la diffusion de documents scientifiques de niveau recherche, publiés ou non, émanant des établissements d'enseignement et de recherche français ou étrangers, des laboratoires publics ou privés.

Measurement of Correlations between Pions from Different W's in $e^+e^- \rightarrow W^+W^-$ Events

DELPHI Collaboration

Abstract

Correlations between pions from different Ws in $e^+e^- \rightarrow W^+W^-$ events are studied using data collected by the DELPHI detector at LEP running at a centre-of-mass energy of 172 GeV in 1996. At the present level of statistics, no enhancement of the correlation function above that expected from a pair of uncorrelated Ws is observed at small values of the four-momentum difference of the pions.

(To be submitted to Physics Letters B)

P. Abreu²¹, W. Adam⁴⁹, T. Adye³⁶, I. Ajinenko⁴¹, G. D. Alekseev¹⁶, R. Alemany⁴⁸, P. P. Allport²², S. Almeded²⁴, U. Amaldi⁹, S. Amato⁴⁶, P. Andersson⁴³, A. Andreazza⁹, P. Antilogus⁹, W.-D. Apel¹⁷, B. Åsman⁴³, J.-E. Augustin²⁵, A. Augustinus³⁰, P. Baillon⁹, P. Bambade¹⁹, F. Barao²¹, M. Barbi⁴⁶, G. Barbiellini⁴⁵, D. Y. Bardin¹⁶, G. Barker⁹, A. Baroncelli³⁹, O. Barring²⁴, M. J. Bates³⁶, M. Battaglia¹⁵, M. Baubillier²³, J. Baudot³⁸, K.-H. Becks⁵¹, M. Begalli⁶, P. Beilliere⁸, Yu. Belokopytov^{9,52}, K. Belous⁴¹, A. C. Benvenuti⁵, M. Berggren⁴⁶, D. Bertini²⁵, D. Bertrand², M. Besancon³⁸, F. Bianchi⁴⁴, M. Bigi⁴⁴, M. S. Bilenky¹⁶, P. Billoir²³, M.-A. Bizouard¹⁹, D. Bloch¹⁰, M. Blume⁵¹, M. Bonesini²⁷, W. Bonivento²⁷, P. S. L. Booth²², A. W. Borgland⁴, G. Borisov^{38,41}, C. Bosio³⁹, O. Botner⁴⁷, E. Boudinov³⁰, B. Bouquet¹⁹, C. Bourdarios¹⁹, T. J. V. Bowcock²², I. Bozovic¹¹, M. Bozzo¹³, P. Branchini³⁹, K. D. Brand³⁵, T. Brenke⁵¹, R. A. Brenner⁴⁷, C. Bricman², R. C. A. Brown⁹, P. Bruckman¹⁸, J.-M. Brunet⁸, L. Bugge³², T. Buran³², T. Burgsmueller⁵¹, P. Buschmann⁵¹, S. Cabrera⁴⁸, M. Caccia²⁷, M. Calvi²⁷, A. J. Camacho Rozas⁴⁰, T. Camporesi⁹, V. Canale³⁷, M. Canepa¹³, F. Cao², F. Carena⁹, L. Carroll²², C. Caso¹³, M. V. Castillo Gimenez⁴⁸, A. Cattai⁹, F. R. Cavallo⁵, V. Chabaud⁹, M. Chapkin⁴¹, Ph. Charpentier⁹, L. Chaussard²⁵, P. Checchia³⁵, G. A. Chelkov¹⁶, M. Chen², R. Chierici⁴⁴, P. Chochula⁷, V. Chorowicz²⁵, V. Cindro⁴², P. Collins⁹, R. Contri¹³, E. Cortina⁴⁸, G. Cosme¹⁹, F. Cossutti⁴⁵, J.-H. Cowell²², H. B. Crawley¹, D. Crennell³⁶, G. Crosetti¹³, J. Cuevas Maestro³³, S. Czellar¹⁵, J. Dahm⁵¹, B. Dalmagne¹⁹, M. Dam²⁸, G. Damgaard²⁸, P. D. Dauncey³⁶, M. Davenport⁹, W. Da Silva²³, A. Deghorain², G. Della Ricca⁴⁵, P. Delpierre²⁶, N. Demaria³⁴, A. De Angelis⁹, W. De Boer¹⁷, S. De Brabandere², C. De Clercq², C. De La Vaissiere²³, B. De Lotto⁴⁵, A. De Min³⁵, L. De Paula⁴⁶, H. Dijkstra⁹, L. Di Ciaccio³⁷, A. Di Diodato³⁷, A. Djannati⁸, J. Dolbeau⁸, K. Doroba⁵⁰, M. Dracos¹⁰, J. Drees⁵¹, K.-A. Drees⁵¹, M. Dris³¹, J.-D. Durand^{25,9}, D. Edsall¹, R. Ehret¹⁷, G. Eigen⁴, T. Ekelof⁴⁷, G. Ekspong⁴³, M. Elsing⁹, J.-P. Engel¹⁰, B. Erzen⁴², M. Espirito Santo²¹, E. Falk²⁴, G. Fanourakis¹¹, D. Fassouliotis⁴⁵, M. Feindt⁹, A. Fenyuk⁴¹, P. Ferrari²⁷, A. Ferrer⁴⁸, S. Fichet²³, T. A. Filippas³¹, A. Firestone¹, P.-A. Fischer¹⁰, H. Foeth⁹, E. Fokitis³¹, F. Fontanelli³, F. Formenti⁹, B. Franek³⁶, A. G. Frodesen⁴, R. Fruhwirth⁴⁹, F. Fulda-Quenzer¹⁹, J. Fuster⁴⁸, A. Galloni²², D. Gamba⁴⁴, M. Gandelman⁴⁶, C. Garcia⁴⁸, J. Garcia⁴⁰, C. Gaspar⁹, U. Gasparini³⁵, Ph. Gavellet⁹, E. N. Gazis³¹, D. Gele¹⁰, J.-P. Gerber¹⁰, L. Gerdyukov⁴¹, R. Gokieli⁵⁰, B. Golob⁴², P. Goncalves²¹, G. Gopal³⁶, L. Gorn¹, M. Gorski⁵⁰, Yu. Gouz^{44,52}, V. Gracco¹³, E. Graziani³⁹, C. Green²², A. Greifath⁵¹, P. Gris³⁸, G. Grosdidier¹⁹, K. Grzelak⁵⁰, S. Gumenyuk⁴¹, M. Gunther⁴⁷, J. Guy³⁶, F. Hahn⁹, S. Hahn⁵¹, Z. Hajduk¹⁸, A. Hallgren⁴⁷, K. Hamacher⁵¹, F. J. Harris³⁴, V. Hedberg²⁴, R. Henriques²¹, J. J. Hernandez⁴⁸, P. Herquet², H. Herr⁹, T. L. Hessing³⁴, J.-M. Heuser⁵¹, E. Higon⁴⁸, H. J. Hilke⁹, S.-O. Holmgren⁴³, P. J. Holt³⁴, D. Holthuisen³⁰, S. Hoorelbeke², M. Houlden²², K. Huet², K. Hultqvist⁴³, J. N. Jackson²², R. Jacobsson⁴³, P. Jalocho⁹, R. Janik⁷, Ch. Jarlskog²⁴, G. Jarlskog²⁴, P. Jarry³⁸, B. Jean-Marie¹⁹, E. K. Johansson⁴³, L. Jonsson²⁴, P. Jonsson²⁴, C. Joram⁹, P. Juillot¹⁰, M. Kaiser¹⁷, F. Kapusta²³, K. Karafasoulis¹¹, M. Karlsson⁴³, S. Katsanevas²⁵, E. C. Katsoufis³¹, R. Keranen⁴, Yu. Khokhlov⁴¹, B. A. Khomenko¹⁶, N. N. Khovanski¹⁶, B. King²², N. J. Kjaer³⁰, O. Klapp⁵¹, H. Klein⁹, P. Kluit³⁰, D. Knoblauch¹⁷, P. Kokkinias¹¹, A. Konopliannikov⁴¹, M. Koratzinos⁹, K. Korcyl¹⁸, V. Kostoukhine⁴¹, C. Kourkoumelis³, O. Kouznetsov^{13,16}, M. Kramer⁴⁹, C. Kreuter⁹, I. Kronkvist²⁴, Z. Kruminstein¹⁶, W. Krupinski¹⁸, P. Kubinec⁷, W. Kucewicz¹⁸, K. Kurvinen¹⁵, C. Lacasta⁹, I. Laktineh²⁵, J. W. Lamsa¹, L. Lanceri⁴⁵, D. W. Lane¹, P. Langefeld⁵¹, J.-P. Laugier³⁸, R. Lauhakangas¹⁵, G. Leder⁴⁹, F. Ledroit¹⁴, V. Lefebvre², C. K. Legan¹, A. Leisos¹¹, R. Leitner²⁹, J. Lemonne², G. Lenzen⁵¹, V. Lepeltier¹⁹, T. Lesiak¹⁸, J. Libby³⁴, D. Liko⁹, R. Lindner⁵¹, A. Lipniacka⁴³, I. Lippi³⁵, B. Loerstad²⁴, J. G. Loken³⁴, J. M. Lopez⁴⁰, D. Loukas¹¹, P. Lutz³⁸, L. Lyons³⁴, J. MacNaughton⁴⁹, G. Maehlum¹⁷, J. R. Mahon⁶, A. Maio²¹, T. G. M. Malmgren⁴³, V. Malychiev¹⁶, F. Mandl⁴⁹, J. Marco⁴⁰, R. Marco⁴⁰, B. Marechal⁴⁶, M. Margoni³⁵, J.-C. Marin⁹, C. Mariotti⁹, A. Markou¹¹, C. Martinez-Rivero³³, F. Martinez-Vidal⁴⁸, S. Marti i Garcia²², F. Matorras⁴⁰, C. Matteuzzi²⁷, G. Matthiae³⁷, M. Mazzucato³⁵, M. Mc Cubbin²², R. Mc Kay¹, R. Mc Nulty⁹, J. Medbo⁴⁷, M. Merk³⁰, C. Meroni²⁷, S. Meyer¹⁷, W. T. Meyer¹, M. Michelotto³⁵, E. Migliore⁴⁴, L. Mirabito²⁵, W. A. Mitaroff⁴⁹, U. Mjoernmark²⁴, T. Moe⁴³, R. Moeller²⁸, K. Moenig⁹, M. R. Monge¹³, P. Moretti¹³, H. Mueller¹⁷, K. Muenich⁵¹, M. Mulders³⁰, L. M. Mundim⁶, W. J. Murray³⁶, B. Muryn^{14,18}, G. Myatt³⁴, F. Naraghi¹⁴, F. L. Navarria⁵, S. Navas⁴⁸, K. Nawrocki⁵⁰, P. Negri²⁷, S. Nemecek¹², W. Neumann⁵¹, N. Neumeister⁴⁹, R. Nicolaidou³, B. S. Nielsen²⁸, M. Nieuwenhuizen³⁰, V. Nikolaenko¹⁰, M. Nikolenko^{10,16}, P. Niss⁴³, A. Nomerotski³⁵, A. Normand³⁴, M. Novak¹², W. Oberschulte-Beckmann¹⁷, V. Obraztsov⁴¹, A. G. Olshevski¹⁶, A. Onofre²¹, R. Orava¹⁵, G. Orazi¹⁰, K. Osterberg¹⁵, A. Ouraou³⁸, P. Paganini¹⁹, M. Paganoni^{9,27}, P. Pages¹⁰, R. Pain²³, H. Palka¹⁸, Th. D. Papadopoulou³¹, K. Papageorgiou¹¹, L. Pape⁹, C. Parkes³⁴, F. Parodi¹³, A. Passeri³⁹, M. Pegoraro³⁵, L. Peralta²¹, H. Pernegger⁴⁹, M. Pernicka⁴⁹, A. Perrotta⁵, C. Petridou⁴⁵, A. Petrolini¹³, H. T. Phillips³⁶, G. Piana¹³, F. Pierre³⁸, M. Pimenta²¹, T. Podobnik⁴², O. Podobrin⁹, M. E. Pol⁶, G. Polok¹⁸, P. Poropat⁴⁵, V. Pozdniakov¹⁶, P. Privitera³⁷, N. Pukhaeva¹⁶, A. Pullia²⁷, D. Radojicic³⁴, S. Ragazzi²⁷, H. Rahmani³¹, J. Rames¹², P. N. Ratoff²⁰, A. L. Read³², M. Reale⁵¹, P. Rebecchi¹⁹, N. G. Redaelli²⁷, M. Regler⁴⁹, D. Reid⁹, R. Reinhardt⁵¹, P. B. Renton³⁴, L. K. Resvanis³, F. Richard¹⁹, J. Richardson²², J. Ridky¹², G. Rinaudo⁴⁴, A. Romero⁴⁴, I. Roncagliolo¹³, P. Ronchese³⁵, V. Ronjin⁴¹, L. Roos²³, E. I. Rosenberg¹, P. Roudeau¹⁹, T. Rovelli⁵, V. Ruhlmann-Kleider³⁸, A. Ruiz⁴⁰, K. Rybicki¹⁸, H. Saarikko¹⁵, Y. Sacquin³⁸, A. Sadovsky¹⁶, O. Sahr¹⁴, G. Sajot¹⁴, J. Salt⁴⁸, M. Sannino¹³, H. Schneider¹⁷, U. Schwickerath¹⁷, M. A. E. Schyns⁵¹, G. Sciolla⁴⁴, F. Scuri⁴⁵, P. Seager²⁰, Y. Sedkykh¹⁶, A. M. Segar³⁴, A. Seitz¹⁷, R. Sekulin³⁶, L. Serbelloni³⁷, R. C. Shellard⁶, P. Siegrist^{9,38}, R. Silvestre³⁸, F. Simonetto³⁵, A. N. Sisakian¹⁶, B. Sitar⁷, T. B. Skaali³², G. Smadja²⁵, O. Smirnova²⁴, G. R. Smith³⁶, O. Solovianov⁴¹, R. Sosnowski⁵⁰, D. Souza-Santos⁶, T. Spassov²¹, E. Spiriti³⁹, P. Sponholz⁵¹, S. Squarcia¹³, D. Stampfer⁹, C. Stanescu³⁹, S. Stanic⁴², S. Stapnes³², I. Stavitski³⁵, K. Stevenson³⁴, A. Stocchi¹⁹, J. Strauss⁴⁹, R. Strub¹⁰, B. Stugu⁴, M. Szczekowski⁵⁰, M. Szeptycka⁵⁰, T. Tabarelli²⁷, J. P. Tavernet²³, E. Tcherniaev⁴¹, O. Tchikilev⁴¹

F.Tegenfeldt⁴⁷, F.Terranova²⁷, J.Thomas³⁴, A.Tilquin²⁶, J.Timmermans³⁰, L.G.Tkatchev¹⁶, T.Todorov¹⁰, S.Todorova¹⁰, D.Z.Toet³⁰, A.Tomaradze², B.Tome²¹, A.Tonazzo²⁷, L.Tortora³⁹, G.Transtromer²⁴, D.Treille⁹, G.Tristram⁸, A.Trombini¹⁹, C.Troncon²⁷, A.Tsirou⁹, M-L.Turluer³⁸, I.A.Tyapkin¹⁶, M.Tyndel³⁶, S.Tzamarias¹¹, B.Ueberschaer⁵¹, O.Ullaland⁹, G.Valenti⁵, E.Vallazza⁴⁵, C.Vander Velde², G.W.Van Apeldoorn³⁰, P.Van Dam³⁰, W.K.Van Doninck², J.Van Eldik³⁰, A.Van Lysebetten², N.Vassilopoulos³⁴, G.Vegni²⁷, L.Ventura³⁵, W.Venus³⁶, F.Verbeure², M.Verlato³⁵, L.S.Vertogradov¹⁶, D.Vilanova³⁸, P.Vincent²⁵, L.Vitale⁴⁵, A.S.Vodopyanov¹⁶, V.Vrba¹², H.Wahlen⁵¹, C.Walck⁴³, P.Weilhammer⁹, C.Weiser¹⁷, A.M.Wetherell⁹, D.Wicke⁵¹, J.H.Wickens², M.Wielers¹⁷, G.R.Wilkinson⁹, W.S.C.Williams³⁴, M.Winter¹⁰, M.Witek¹⁸, T.Wlodek¹⁹, J.Yi¹, K.Yip³⁴, O.Yushchenko⁴¹, F.Zach²⁵, A.Zaitsev⁴¹, A.Zalewska⁹, P.Zalewski⁵⁰, D.Zavrtanik⁴², E.Zevgolatakos¹¹, N.I.Zimin¹⁶, D.Zontar⁴², G.C.Zucchelli⁴³, G.Zumerle³⁵

¹Department of Physics and Astronomy, Iowa State University, Ames IA 50011-3160, USA

²Physics Department, Univ. Instelling Antwerpen, Universiteitsplein 1, B-2610 Wilrijk, Belgium and IIHE, ULB-VUB, Pleinlaan 2, B-1050 Brussels, Belgium

and Faculté des Sciences, Univ. de l'Etat Mons, Av. Maistriau 19, B-7000 Mons, Belgium

³Physics Laboratory, University of Athens, Solonos Str. 104, GR-10680 Athens, Greece

⁴Department of Physics, University of Bergen, Allégaten 55, N-5007 Bergen, Norway

⁵Dipartimento di Fisica, Università di Bologna and INFN, Via Irnerio 46, I-40126 Bologna, Italy

⁶Centro Brasileiro de Pesquisas Físicas, rua Xavier Sigaud 150, RJ-22290 Rio de Janeiro, Brazil and Depto. de Física, Pont. Univ. Católica, C.P. 38071 RJ-22453 Rio de Janeiro, Brazil

and Inst. de Física, Univ. Estadual do Rio de Janeiro, rua São Francisco Xavier 524, Rio de Janeiro, Brazil

⁷Comenius University, Faculty of Mathematics and Physics, Mlynska Dolina, SK-84215 Bratislava, Slovakia

⁸Collège de France, Lab. de Physique Corpusculaire, IN2P3-CNRS, F-75231 Paris Cedex 05, France

⁹CERN, CH-1211 Geneva 23, Switzerland

¹⁰Centre de Recherche Nucléaire, IN2P3 - CNRS/ULP - BP20, F-67037 Strasbourg Cedex, France

¹¹Institute of Nuclear Physics, N.C.S.R. Demokritos, P.O. Box 60228, GR-15310 Athens, Greece

¹²FZU, Inst. of Physics of the C.A.S. High Energy Physics Division, Na Slovance 2, 180 40, Praha 8, Czech Republic

¹³Dipartimento di Fisica, Università di Genova and INFN, Via Dodecaneso 33, I-16146 Genova, Italy

¹⁴Institut des Sciences Nucléaires, IN2P3-CNRS, Université de Grenoble 1, F-38026 Grenoble Cedex, France

¹⁵Helsinki Institute of Physics, HIP, P.O. Box 9, FIN-00014 Helsinki, Finland

¹⁶Joint Institute for Nuclear Research, Dubna, Head Post Office, P.O. Box 79, 101 000 Moscow, Russian Federation

¹⁷Institut für Experimentelle Kernphysik, Universität Karlsruhe, Postfach 6980, D-76128 Karlsruhe, Germany

¹⁸Institute of Nuclear Physics and University of Mining and Metallurgy, Ul. Kawiory 26a, PL-30055 Krakow, Poland

¹⁹Université de Paris-Sud, Lab. de l'Accélérateur Linéaire, IN2P3-CNRS, Bât. 200, F-91405 Orsay Cedex, France

²⁰School of Physics and Chemistry, University of Lancaster, Lancaster LA1 4YB, UK

²¹LIP, IST, FCUL - Av. Elias Garcia, 14-1º, P-1000 Lisboa Codex, Portugal

²²Department of Physics, University of Liverpool, P.O. Box 147, Liverpool L69 3BX, UK

²³LPNHE, IN2P3-CNRS, Universités Paris VI et VII, Tour 33 (RdC), 4 place Jussieu, F-75252 Paris Cedex 05, France

²⁴Department of Physics, University of Lund, Sölvegatan 14, S-22363 Lund, Sweden

²⁵Université Claude Bernard de Lyon, IPNL, IN2P3-CNRS, F-69622 Villeurbanne Cedex, France

²⁶Univ. d'Aix - Marseille II - CPP, IN2P3-CNRS, F-13288 Marseille Cedex 09, France

²⁷Dipartimento di Fisica, Università di Milano and INFN, Via Celoria 16, I-20133 Milan, Italy

²⁸Niels Bohr Institute, Blegdamsvej 17, DK-2100 Copenhagen 0, Denmark

²⁹NC, Nuclear Centre of MFF, Charles University, Areal MFF, V Holesovickach 2, 180 00, Praha 8, Czech Republic

³⁰NIKHEF, Postbus 41882, NL-1009 DB Amsterdam, The Netherlands

³¹National Technical University, Physics Department, Zografou Campus, GR-15773 Athens, Greece

³²Physics Department, University of Oslo, Blindern, N-1000 Oslo 3, Norway

³³Dpto. Física, Univ. Oviedo, Avda. Calvo Sotelo, S/N-33007 Oviedo, Spain, (CICYT-AEN96-1681)

³⁴Department of Physics, University of Oxford, Keble Road, Oxford OX1 3RH, UK

³⁵Dipartimento di Fisica, Università di Padova and INFN, Via Marzolo 8, I-35131 Padua, Italy

³⁶Rutherford Appleton Laboratory, Chilton, Didcot OX11 0QX, UK

³⁷Dipartimento di Fisica, Università di Roma II and INFN, Tor Vergata, I-00173 Rome, Italy

³⁸CEA, DAPNIA/Service de Physique des Particules, CE-Saclay, F-91191 Gif-sur-Yvette Cedex, France

³⁹Istituto Superiore di Sanità, Ist. Naz. di Fisica Nucl. (INFN), Viale Regina Elena 299, I-00161 Rome, Italy

⁴⁰Instituto de Física de Cantabria (CSIC-UC), Avda. los Castros, S/N-39006 Santander, Spain, (CICYT-AEN96-1681)

⁴¹Inst. for High Energy Physics, Serpukov P.O. Box 35, Protvino, (Moscow Region), Russian Federation

⁴²J. Stefan Institute, Jamova 39, SI-1000 Ljubljana, Slovenia and Department of Astroparticle Physics, School of Environmental Sciences, Kostanjevska 16a, Nova Gorica, SI-5000 Slovenia, and Department of Physics, University of Ljubljana, SI-1000 Ljubljana, Slovenia

⁴³Fysikum, Stockholm University, Box 6730, S-113 85 Stockholm, Sweden

⁴⁴Dipartimento di Fisica Sperimentale, Università di Torino and INFN, Via P. Giuria 1, I-10125 Turin, Italy

⁴⁵Dipartimento di Fisica, Università di Trieste and INFN, Via A. Valerio 2, I-34127 Trieste, Italy and Istituto di Fisica, Università di Udine, I-33100 Udine, Italy

⁴⁶Univ. Federal do Rio de Janeiro, C.P. 68528 Cidade Univ., Ilha do Fundão BR-21945-970 Rio de Janeiro, Brazil

⁴⁷Department of Radiation Sciences, University of Uppsala, P.O. Box 535, S-751 21 Uppsala, Sweden

⁴⁸IFIC, Valencia-CSIC, and D.F.A.M.N., U. de Valencia, Avda. Dr. Moliner 50, E-46100 Burjassot (Valencia), Spain

⁴⁹Institut für Hochenergiephysik, Österr. Akad. d. Wissensch., Nikolsdorfergasse 18, A-1050 Vienna, Austria

⁵⁰Inst. Nuclear Studies and University of Warsaw, Ul. Hoza 69, PL-00681 Warsaw, Poland

⁵¹Fachbereich Physik, University of Wuppertal, Postfach 100 127, D-42097 Wuppertal, Germany

⁵²On leave of absence from IHEP Serpukhov

1 Introduction

The fragmentation of quarks and gluons into hadrons is not calculable in QCD. Instead, phenomenological models are used to describe the hadronization process [1]. The models are built according to a probabilistic scheme, while the correct theory is an amplitude-based quantum mechanical description.

For a pair of identical bosons, the quantum mechanical wave-function must be symmetric under particle exchange, which leads to an enhancement in the production of pairs of bosons of the same charge and similar momenta. Such effects are observed in a variety of processes [2] and are attributed to this Bose-Einstein symmetrization. Since a symmetrization of amplitudes is normally absent in probabilistic descriptions, a crucial question is whether or not Bose-Einstein correlations can be considered to be a small correction to the probabilistic approach to the hadronization processes. If not, models formulated along a probabilistic approach would be far from reality [3]. There are clear indications that Bose-Einstein effects play an increasingly large role with increasing centre-of-mass energy and it is becoming difficult to perform detailed analyses of multiparticle production without a better understanding of this effect. An experimental example is the distortion by Bose-Einstein correlations of the Breit-Wigner shape for oppositely charged pions from the decay of broad resonances, observed at LEP1 energies [4,5] (see also [6]).

Recently, it has also been conjectured that the measurement of the W mass at LEP2 by reconstructing W pairs giving 4 jets is likely to be affected by Bose-Einstein correlations between pions from different W s [3]. The typical separation in space and time between the W^+ and W^- in $e^+e^- \rightarrow W^+W^-$ events is smaller than 0.1 fm at LEP2 energies, much smaller than the source radii of 0.5 fm usually observed, and consequently pions from different W s can be subject to Bose-Einstein symmetrization. A study of the correlations between pions originating from different W s presents a unique possibility of measuring, in a clean way, the Bose-Einstein effect between particles from different, well-understood, sources. Such measurements may help to provide a better understanding of the Bose-Einstein phenomenon and, correspondingly, lead to improvement of existing models or the need for new models to describe multiparticle production.

This paper describes an investigation of Bose-Einstein correlations between pions from different W s in $e^+e^- \rightarrow W^+W^-$ events at a centre-of-mass energy of 172 GeV, using data collected with the DELPHI detector [7,8] at LEP in 1996.

2 Analysis

To study the enhanced probability for emission of two identical bosons, the correlation function R is defined as

$$R(p_1, p_2) = \frac{P(p_1, p_2)}{P_0(p_1, p_2)}, \quad (1)$$

where $P(p_1, p_2)$ is the two-particle probability density, subject to Bose-Einstein symmetrization, p_i is the four-momentum of particle i , and $P_0(p_1, p_2)$ is a reference two-particle distribution which, ideally, resembles $P(p_1, p_2)$ in all respects, apart from the lack of Bose-Einstein symmetrization.

If $f(x)$ is the space-time distribution of the source, $R(p_1, p_2)$ takes the form

$$R(p_1, p_2) = 1 + |G[f(x)]|^2,$$

where $G[f(x)] = \int f(x)e^{-i(p_1-p_2)\cdot x} dx$ is the Fourier transform of $f(x)$. Thus, by studying the correlations between the momenta of pion pairs, one can determine the distribution of the points of origin of the pions. Experimentally, it has been observed [9] that the effect can be described in terms of the variable Q , defined by $Q^2 = M^2(\pi\pi) - 4m_\pi^2$, where M is the invariant mass of the two pions. The correlation function can then be written as

$$R(Q) = \frac{P(Q)}{P_0(Q)}, \quad (2)$$

which is often parametrized by the function

$$R(Q) = 1 + \lambda e^{-r^2 Q^2}, \quad (3)$$

where the parameter r gives the source size and λ the strength of the correlation between the pions.

For the present analysis of correlations between like-sign pions from different W s, the two-particle distribution of unlike-sign charged pions coming from different W s is used as the reference two-particle distribution $P_0(Q)$.

Unlike-sign two-particle distributions are generally strongly influenced by decays such as η into $\pi^+\pi^-\pi^0$ or $\pi^+\pi^-\gamma$, or ω into $\pi^+\pi^-\pi^0$. However, in the present case, when the pions come from different W s, the unlike-sign two-particle distribution may represent an ideal reference, provided colour reconnection effects are not large. This is because, in the absence of colour reconnection, it should be identical to the like-sign distribution except for Bose-Einstein correlation effects, and should not contain pairs from decays of particles or resonances.

To obtain the two-particle Q distribution for pairs of pions coming from different W s, the following procedure was used. The Q distribution for pion pairs was obtained for $e^+e^- \rightarrow W^+W^-$ events with fully hadronic decays, i.e. events where both W s decay into two quark jets. This distribution is the sum of the distribution of pion pairs coming from the same W and that of pion pairs coming from different W s. The contribution of pairs coming from the same W was subtracted statistically, using the Q distribution obtained from $e^+e^- \rightarrow W^+W^-$ events in which one W decays into two quarks and the other one into lepton plus neutrino. The same procedure was followed for both like-sign and unlike-sign pion pairs to obtain $P(Q)$ and $P_0(Q)$, respectively.

The detector effects on the analysis were estimated using samples of WW and background events generated with PYTHIA 5.7 [10] with the fragmentation tuned to the DELPHI data at LEP1 [11]. The generated events were passed through the full detector simulation program DELSIM [8].

3 Particle and Event Selections

The track and event selections, which are described below, were similar to those in [12].

3.1 Particle Selection

The DELPHI detector and its performance have been described in [7,8]. The analysis relied on the information provided by the tracking detectors: the Micro-vertex Detector, the Inner Detector, the Time Projection Chamber as main tracking detector, the Outer Detector, the Forward Chambers and the Muon Chambers. Neutral particles were detected from their electro-magnetic showers in the High density Projection Chamber, the

Forward Electro-Magnetic Chambers and the luminosity monitor, STIC; neutral hadronic showers were measured in the instrumented iron return yoke of the solenoidal magnet.

All charged particles except those tagged as hard leptons in semileptonic events were taken to be pions. Charged particles were selected if they fulfilled the following criteria :

- polar angle between 10° and 170° ;
- momentum greater than $0.1 \text{ GeV}/c$ and smaller than the beam momentum;
- good quality, assessed as follows:
 - track length greater than 15 cm ;
 - impact parameters with respect to the nominal interaction point less than 4 cm (transverse and longitudinal with respect to the beam direction);
 - error on momentum measurement less than 100% .

For neutral particles the following selection criteria were applied :

- energy of the electromagnetic or hadron shower greater than 0.5 GeV ;
- additional requirements on shower quality, assessed as follows:
 - showers in the STIC must have deposits in more than one cell;
 - showers in the hadron calorimeter must have an error in the energy of less than 100% .

Electron identification was performed in the polar angle range between 20° and 160° by looking for characteristic energy deposition in the central and forward/backward electromagnetic calorimeters and demanding an energy-to-momentum ratio consistent with unity. For this polar angle range the identification efficiency for high momentum electrons was determined from simulation to be $(77 \pm 2)\%$, in good agreement with the efficiency determined using Bhabha events measured in the detector.

Tracks were identified as due to muons if they had at least one associated hit in the muon chambers, or an energy deposition in the hadronic calorimeter consistent with a minimum ionizing particle. Muon identification was performed in the polar angle range between 10° and 170° . Within this acceptance, the identification efficiency was determined from simulation to be $(92 \pm 1)\%$. Good agreement was found between data and simulation for high momentum muons in $Z \rightarrow \mu^+ \mu^-$ decays, and for low momentum pairs produced in $\gamma\gamma$ reactions.

3.2 Event Selection for Fully Hadronic Final States

The event selection criteria were optimised in order to ensure that the final state was purely hadronic and in order to reduce the residual background, for which the dominant contribution is radiative $q\bar{q}$ production, $e^+e^- \rightarrow q\bar{q}(\gamma)$, especially the radiative return to the Z peak, $e^+e^- \rightarrow Z\gamma \rightarrow q\bar{q}\gamma$.

Only events where the value of the thrust was less than 0.9 were considered. For each event passing the above criteria, all particles were clustered into jets using the LUCLUS algorithm [13] with the resolution parameter $d_{\text{join}} = 6.5 \text{ GeV}/c$. At least four jets were required, with more than three particles in each jet.

Events from the radiative return to the Z peak were rejected by requiring the effective centre-of-mass energy of the e^+e^- annihilation to be larger than 115 GeV . The effective energy was estimated using either the recoil mass calculated from one or two isolated photons measured in the detector or, in the absence of such a photon, by forcing a 2-jet interpretation of the event and assuming that a photon had been emitted collinear to the beam line.

Events were then forced into a four-jet configuration. The four-vectors of the jets were used in a kinematic fit, which imposed conservation of energy and momentum and equality of masses of two pairs of jets. Events were used only if at least one of the three possible pairings of jets had a fit probability larger than 2%. The distribution of the fitted mass of the two jets for all those combinations is shown in Fig. 1a, together with the background contribution and the combined expected distribution of the signal and background. The final cut to select WW events was the requirement of a fitted mass larger than $75 \text{ GeV}/c^2$ for at least one retained combination.

From a data sample corresponding to an integrated luminosity of 10 pb^{-1} , 24 events were selected. The purity of the selection, estimated using simulated events, was 90%.

3.3 Event Selection for Mixed Hadronic and Leptonic Final States

Events in which one W decays into lepton plus neutrino and the other one into quarks are characterized by two hadronic jets, one energetic isolated charged lepton, and missing momentum resulting from the neutrino. The main backgrounds to these events are radiative $q\bar{q}$ production and four-fermion final states containing two quarks and two charged leptons of the same flavour.

Events were selected by requiring six or more charged particles and a missing momentum of more than 10% of the total centre-of-mass energy. Electron and muon tags were applied to the events. In $q\bar{q}(\gamma)$ events, the selected lepton candidates are either leptons produced in heavy quark decays or misidentified hadrons, which generally have rather low momenta and small angles with respect to their quark jets. The momentum of the selected muon, or the energy deposited in the electromagnetic calorimeters by the selected electron, was required to be greater than 20 GeV. The energy not associated to the lepton, but assigned instead to other charged or neutral particles in a cone of 10° around the lepton, is a useful measure of the lepton's isolation; this energy was required to be less than 5 GeV for both muons and electrons. In addition, the isolation angle between the lepton and the nearest charged particle with a momentum greater than 1 GeV/c was required to be larger than 10° . If more than one identified lepton passed these cuts, the one with highest momentum was considered to be the lepton candidate from the W decay. The angle between the lepton and the missing momentum vector was required to be greater than 70° . All the other particles were forced into two jets using the LUCLUS algorithm [13]. Both jets had to contain more than two charged particles.

Further suppression of the radiative $q\bar{q}$ background was achieved by looking for evidence of an ISR (Initial State Radiation) photon. Events were removed if there was a cluster with energy deposition greater than 20 GeV in the electromagnetic calorimeters, not associated with a charged particle. Events with ISR photons at small polar angles, where they would be lost inside the beam pipe, were suppressed by requiring the polar angle of the missing momentum vector to satisfy $|\cos \theta_{\text{miss}}| < 0.94$.

The four-fermion neutral current background was reduced by applying additional cuts to events in which a second lepton of the same flavour as the first was detected. Such events were rejected if the energy in a cone of 10° around the second lepton direction was greater than 5 GeV.

If no lepton was identified, the most energetic particle which formed an angle greater than 25° with all other charged particles was considered as a lepton candidate; this recovered some unidentified leptons and some additional $W \rightarrow \tau\nu_\tau$ decays. In this case the lepton was required to have a momentum greater than 20 GeV/c, as before, but

tighter cuts were applied to the amount of missing momentum (greater than 20 GeV/c) and to its polar angle ($|\cos \theta_{\text{miss}}| < 0.85$).

A kinematical fit was performed on the selected events. The four-vectors of the two jets and of the lepton were used in the fit, which imposed conservation of energy and momentum and equality of the masses of the two-jet system and the lepton-neutrino system, attributing the missing momentum of the event to the undetected neutrino. Events were used only if the fit probability was larger than 0.1%. The distribution of the fitted mass for these events is shown in Fig. 1b, together with the background contribution and combined expected signal and background distribution. The final cut, as in the case of fully hadronic final states, was that the fitted mass of the two-jet system had to be larger than 75 GeV.

From the data sample corresponding to an integrated luminosity of 10 pb^{-1} , 25 events were selected. The purity of the selection, estimated using simulated events, was about 98%.

4 Results

Fig. 2a shows the like-sign ($\pi^\pm\pi^\pm$) Q -spectrum for fully hadronic final states (open circles) and for mixed hadronic and leptonic final states (closed circles). The Q distributions for unlike-sign ($\pi^+\pi^-$) pairs for both samples are shown in Fig. 2b. The Q -spectra shown for the mixed decay channel have been normalized to the number of hadronically decaying W candidates in the fully hadronic sample.

For both the like-sign and unlike-sign pion pairs, the maxima of the spectra occur at larger Q values for the fully hadronic decays than for the mixed decays, since two pions from different Ws are less likely to have a small Q value.

To obtain distributions for pion pairs coming from different Ws, the normalised Q distributions of the mixed sample were subtracted from those for the fully hadronic sample, both for the like-sign pairs and for the unlike-sign pairs. The resulting distributions are shown in Fig. 3. In this figure, no excess of like-sign pairs over unlike-sign pairs is observed. The ratio of like-sign to unlike-sign pairs, $R(Q)$, is shown in Fig. 4.

Since no enhancement of the correlation function is observed at low Q values, the parameter r in eq. (3) is not well defined. The fit to the correlation function with expression (3) was therefore performed with a fixed value of $r=0.5 \text{ fm}$, as measured in Z^0 decays [5]. The fit yielded the value:

$$\lambda = -0.20 \pm 0.22 \text{ (stat)} \quad (4)$$

with $\chi^2 = 14$ for 14 degrees of freedom. This fit is shown by the solid curve in Fig. 4. At the present level of statistics, no evidence is observed for Bose-Einstein correlations between pions from *different* Ws.

In Monte-Carlo events with full detector simulation, the contamination of like-sign particle pairs where at least one particle is not a pion is about 18% for the interval $Q < 0.5 \text{ GeV}/c^2$. Correcting for this effect with the same methodology as in [14] would change the value of λ by about -0.04 . As this correction is much less than the statistical error on λ , the parameter value (4) obtained from the fit is used in the following analysis without correcting for this effect.

It has been shown [5] that using the unlike-sign two-particle distributions as reference distribution for Bose-Einstein correlation studies for particles from the decay of the Z^0 yields values for the measured Bose-Einstein parameters which depend strongly on the influence of resonance decays. Therefore, in order to study the correlations between

particles from the *same* W in the two-jet sample, the same methodology as in [5] was used, i.e. the event mixing technique. The values of λ and r obtained were compatible with those found at the $Z^{0\dagger}$.

To estimate the systematic errors on λ in (4), the following procedures were used:

- The selected hadronically decaying WW candidate events contain about 10% background. If the value of λ for the background events was about 0.3, as measured at the Z^0 [14,15], the presence of Bose-Einstein correlations in the background events would have changed the λ value obtained in (4) by +0.06. To estimate any other possible influences of background events, the background contamination estimated from simulation without Bose-Einstein correlations was subtracted from the experimental Q distributions and the analysis was repeated. The change in the value of λ was negligible. Consequently, the systematic error due to background events was taken to be $\Delta\lambda=\pm 0.06$.
- The distribution of $R(Q)$ for simulated events, without Bose-Einstein correlations included, was obtained in exactly the same way as that from the data (this is shown in Fig. 4 as open points). $R(Q)$ for the data was divided by $R(Q)$ of these simulated events, in order to take into account possible detector effects and any correlations which are not due to Bose-Einstein correlations, and the fit to eq. (3) was repeated. The deviation of λ from the value (4) was used as the estimate of the systematic error from this source, $\Delta\lambda=\pm 0.04$.
- Cuts on the charged particle multiplicity were applied to the fully hadronic and leptonic selected events in order to estimate possible uncertainties due to the influence of the events with the lowest or highest multiplicity. The uncertainty from this source was estimated to be ± 0.03 .
- To estimate the influence of final state Coulomb interactions, a correction by the Gamow factor [18] was applied to $R(Q)$. This increased λ by 0.03. However, it has been suggested [19] that the Gamow factor overestimates the size of the final state Coulomb interaction. Hence it was decided not to correct the λ parameter for Coulomb interactions, but to include a systematic error of ± 0.03 on λ due to this source.

Adding all contributions in quadrature gave the final result (for r fixed to 0.5 fm):

$$\lambda = -0.20 \pm 0.22 \text{ (stat)} \pm 0.08 \text{ (syst)}. \quad (5)$$

5 Discussion

In addition to the data points, Fig. 4 also shows $R(Q)$ distributions predicted using WW events generated by PYTHIA.

When no Bose-Einstein effects are included, the correlation function $R(Q)$ is found to be equal to one within errors in the whole Q -region presented, in good agreement with the data. This is true for events passed through the full detector simulation and analysed in the same way as the data (open circles), and also if $R(Q)$ is obtained using only fully hadronically decaying WW events and considering only pairs of pions from different W s (not shown). It is also true if $R(Q)$ is extracted in the same two ways at generator level (also not shown).

[†]The fitted values were $\lambda=0.63\pm 0.23$ and $r=0.55\pm 0.11$ fm. The corresponding values obtained by ALEPH [14] and DELPHI [15] at the Z^0 using the same method (mixed-event reference sample) were $\lambda=0.40\pm 0.02$ and $r=0.50\pm 0.02$ fm and $\lambda=0.35\pm 0.04$ and $r=0.42\pm 0.04$ fm, respectively. At the Z^0 , using unlike-sign pairs for the reference sample has typically given larger values of both λ and r [14–16].

Bose-Einstein correlations can be included in PYTHIA by using the LUBOEI code, where they are introduced as a final state interaction [17]. After the generation of the pion momenta, the values generated for all identical pions are modified by an algorithm that reduces their momentum vector differences. This procedure violates energy-momentum conservation. Finally, rescaling is therefore applied to restore the total energy and momentum. This code has been shown [5] to reproduce the two-particle correlations measured in Z^0 decays well if Bose-Einstein correlations are switched on with a Gaussian parametrization for pions that are produced either promptly or as decay products of short-lived resonances[†] and the parameter values $\lambda = 1$ and $r = 0.5$ fm are used[§]. The value $\lambda=1$ for direct pions corresponds to $\lambda \sim 0.4$ for all pions or $\lambda \sim 0.3$ for all particles [14,15].

The same algorithm with the same values of λ and r was applied to the generated WW events to calculate predictions for the case where Bose-Einstein correlations are present. The $R(Q)$ distributions for pions from different Ws for generated events were again obtained in the same two ways as before, i.e. (a) directly, by using only the fully hadronic decay channel and considering only pairs of pions coming from different Ws, and (b) using the difference between the distributions for fully hadronic and mixed hadronic and leptonic decay channels, as done for the data. The shaded area in Fig. 4 represents the area between the $R(Q)$ distributions obtained in these two ways. In the low- Q region, procedure (a) gave the lower values of $R(Q)$, and the $R(Q)$ distribution for fully simulated events was again consistent with that obtained at generator level.

Fig. 4 also shows curves obtained by fitting the $R(Q)$ for like-sign particles measured by DELPHI [5] and ALEPH [14] at the Z^0 using the event mixing technique (dashed and dotted curves, respectively). These $R(Q)$ distributions measured in Z^0 decays show a clear enhancement in the low- Q region. The statistical errors are negligible.

The $R(Q)$ distribution for like-sign pions from different Ws (closed circles in Fig. 4) in the low- Q region is systematically below the predictions including Bose-Einstein effects and the fits to Z^0 data, and does not show any enhancement. However, at this level of statistics no conclusion can yet be drawn.

6 Summary

The first measurement of the correlation function for like-sign particles arising from *different* Ws is reported, using unlike-sign particles as a reference. The Q distributions of pion pairs from different Ws, both for like-sign and for unlike-sign combinations, were obtained statistically, as the difference between (a) the distribution for all combinations in fully hadronically decaying WW (four jet) events and (b) the appropriately normalized distribution for events where one of the Ws decays leptonically (two jet, lepton, neutrino events). Interpreting this difference in the above terms assumes that colour reconnection effects are not too large. At the present level of statistical precision, no enhancement of the correlation function is observed at small Q values. Fixing the value of the radius r at 0.5 fm, the Bose-Einstein correlation strength is found to be

$$\lambda = -0.20 \pm 0.22 \text{ (stat)} \pm 0.08 \text{ (syst)}. \quad (6)$$

[†]Resonances with longer lifetime than the K^* (890) were considered long-lived.

[§]The measured values of the parameters for such 'direct' pions in Z^0 decays were $\lambda = 1.06 \pm 0.17$, $r = 0.49 \pm 0.05$ fm [5].

Acknowledgments

We thank T. Sjöstrand for very useful discussions. We are greatly indebted to our technical collaborators and to the funding agencies for their support in building and operating the DELPHI detector, and to the members of the CERN-SL Division for the excellent performance of the LEP collider.

References

- [1] B. Andersson, G. Gustafson, G. Ingelman and T. Sjöstrand, Phys. Rep. **97** (1983) 243;
B.R. Webber, Nucl. Phys. **B238** (1984) 492.
- [2] A. Tomaradze, *Results on Bose-Einstein correlations*, Proc. 7th Intern. Workshop on Multiparticle Production “Correlations and Fluctuations”, Nijmegen 1996, eds. R.C. Hwa et al., WSPC, Singapore, 1997, p. 34;
B. Lörstad, Int. J. Mod. Phys. **A4** (1989) 2861;
S. Haywood, *Where are we going with Bose-Einstein – A mini review*, RAL Report 94-074.
- [3] L. Lönnblad and T. Sjöstrand, Phys. Lett. **B351** (1995) 293.
- [4] P.D. Acton et al. (OPAL Coll.), Z. Phys. **C56** (1992) 521;
P. Abreu et al. (DELPHI Coll.), Z. Phys. **C65** (1995) 587.
- [5] P. Abreu et al. (DELPHI Coll.), Z. Phys. **C63** (1994) 17.
- [6] G. Lafferty, Z. Phys. **C60** (1993) 659;
- [7] P. Aarnio et al. (DELPHI Coll.), Nucl. Instr. & Meth. **A303** (1991) 233.
- [8] P. Abreu et al. (DELPHI Coll.), Nucl. Instr. & Meth. **A378** (1996) 57.
- [9] E.A. De Wolf, I. Dremin and W. Kittel, Phys. Reports **270** (1996) 1.
- [10] T. Sjöstrand, Comp. Phys. Comm. **82** (1994) 74.
- [11] P. Abreu et al. (DELPHI Coll.), Z. Phys. **C73** (1996) 11.
- [12] P. Abreu et al. (DELPHI Coll.), *Measurement and interpretation of the W-pair cross-section in e^+e^- interactions at 161 GeV*, CERN-PPE 97-09, to appear in Phys. Lett. B.
- [13] T. Sjöstrand, *PYTHIA 5.7 / JETSET 7.4*, CERN-TH.7112/93 (1993).
- [14] D. Decamp et al. (ALEPH Coll.), Z. Phys. **C54** (1992) 75.
- [15] P. Abreu et al. (DELPHI Coll.), Phys. Lett. **B286** (1992) 201
- [16] G. Alexander et al., (OPAL Coll.), Z. Phys. **C72** (1996) 389.
- [17] T. Sjöstrand, Comp. Phys. Comm. **27** (1982) 243; *ibid.* **28** (1983) 229;
T. Sjöstrand and M. Bengtsson, Comp. Phys. Comm. **43** (1987) 367.
- [18] M. Gyulassy, S.K. Kaufmann and L.W. Wilson, Phys. Rev. **C20** (1979) 2267.
- [19] M.G. Bowler, Phys. Lett. **B270** (1991) 69.

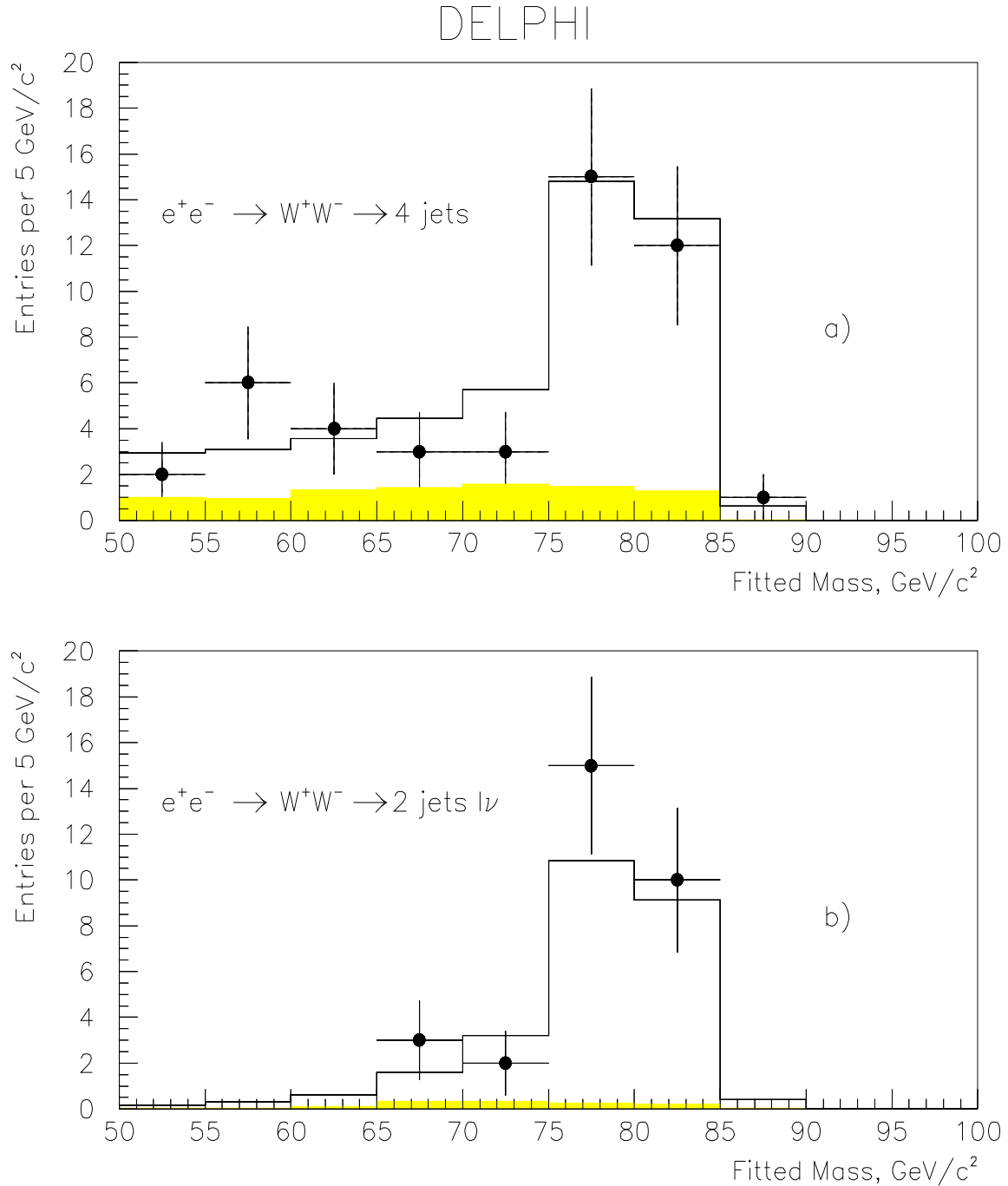


Figure 1: Reconstructed W mass distribution obtained from the kinematic fit described in the text for (a) fully hadronic (4-jet) final states and (b) mixed hadronic and leptonic (jet-jet-lepton-neutrino) final states. For fully hadronic (4-jet) final states all combinations are plotted for which the fit probability was larger than 2%. The shaded areas represent the background contributions (negligible for mixed final states). The histograms are the sum of the expected signal and background.

DELPHI

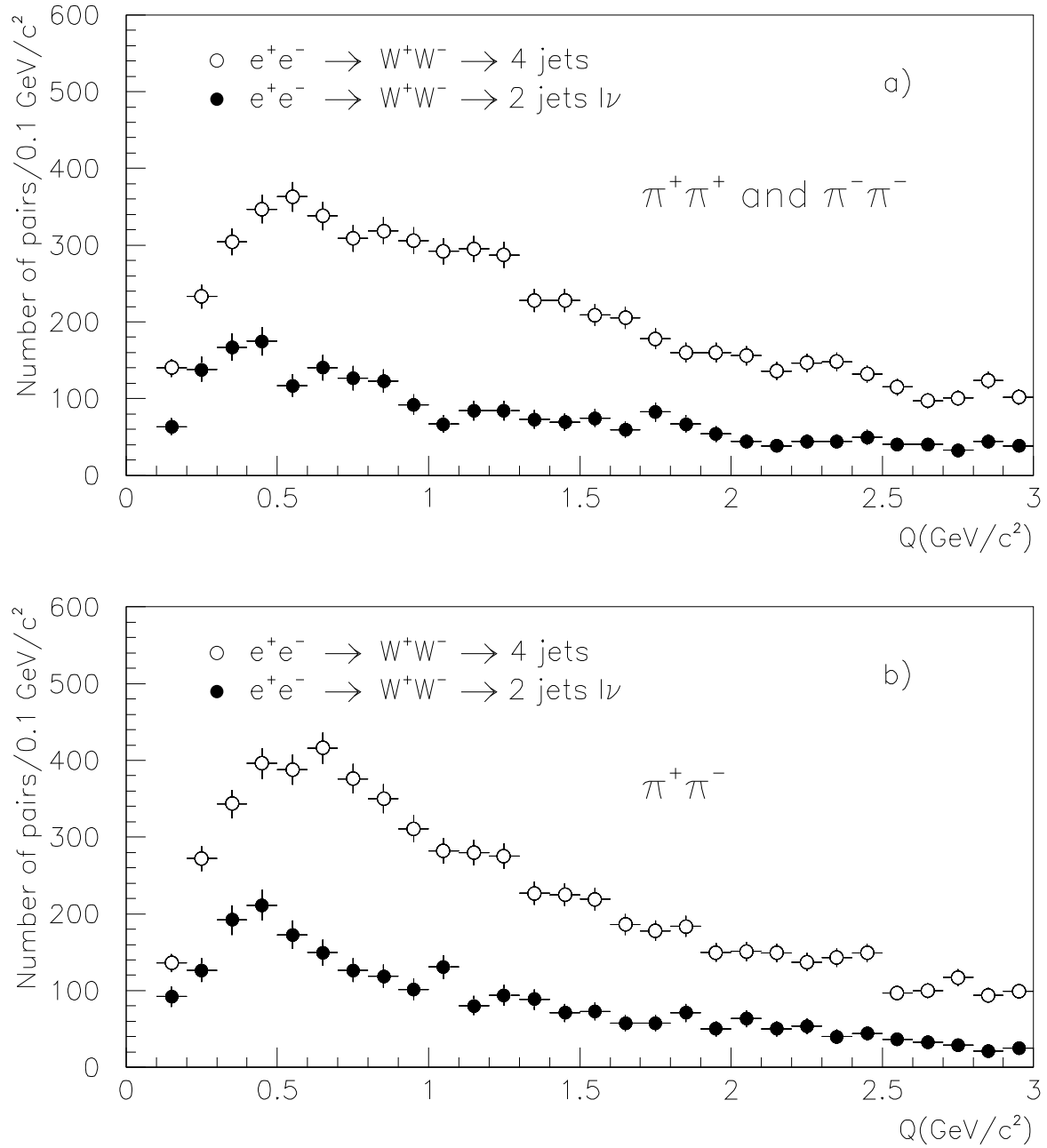


Figure 2: Q distributions for like-sign (a) and unlike-sign (b) pairs for fully hadronic final states (*open circles*) and mixed hadronic and leptonic final states (*closed circles*). The Q distributions for the mixed decay channel have been normalized to the number of selected hadronically decaying W candidates present in the fully hadronic channel (see text).

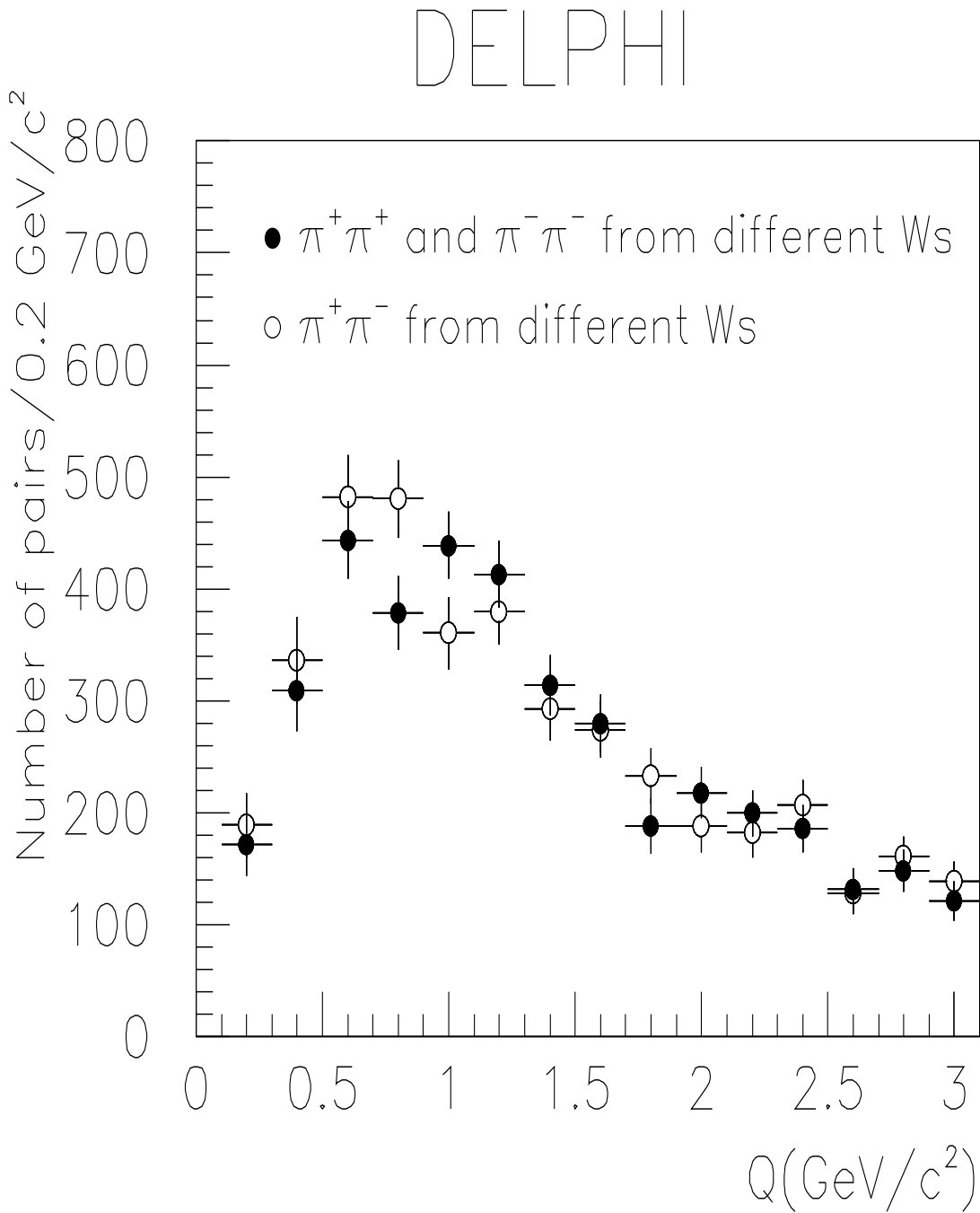


Figure 3: Q distributions for like-sign (*closed circles*) and unlike-sign (*open circles*) pairs for pions arising from different Ws.

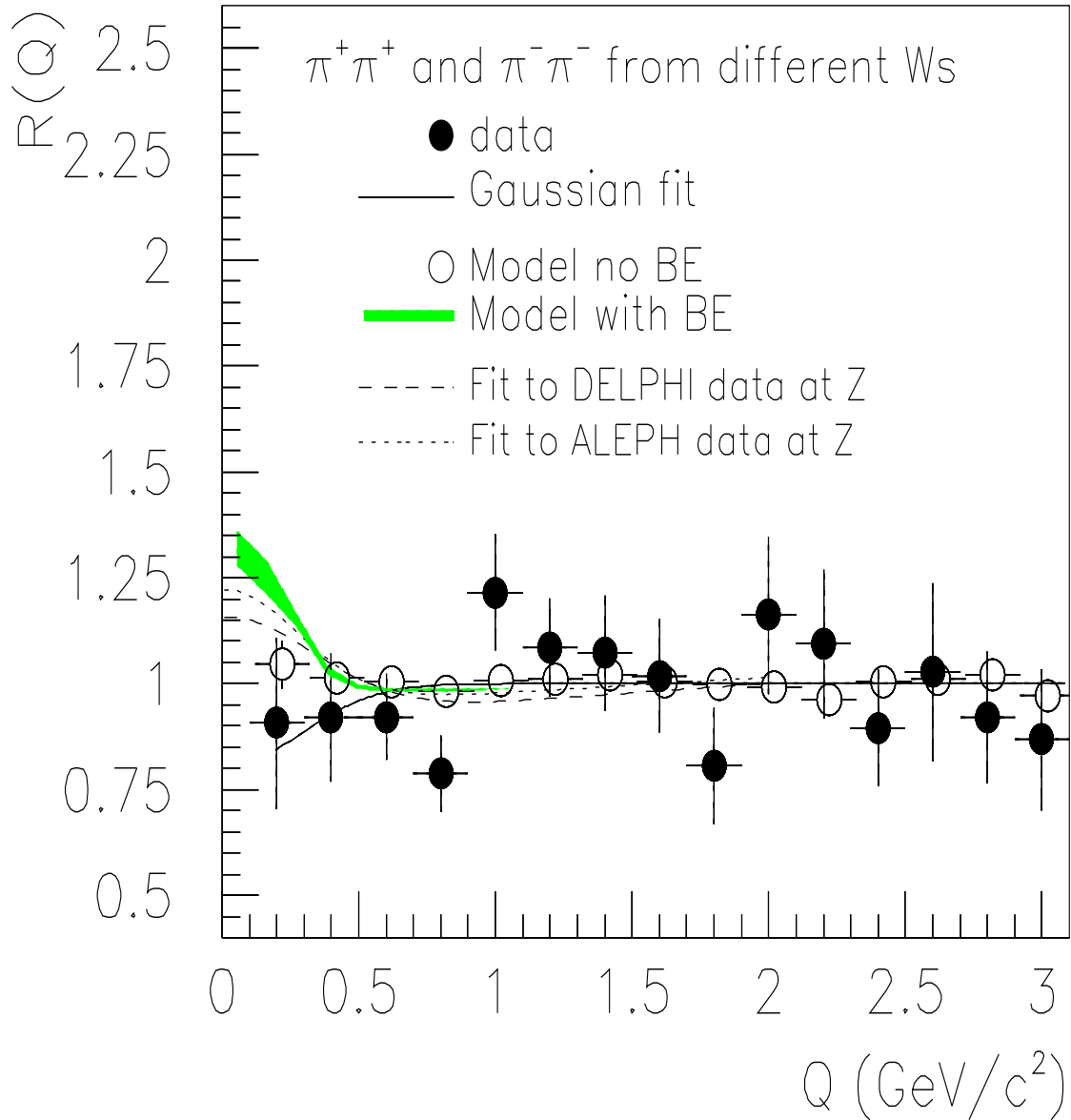
DELPHI $e^+e^- \rightarrow W^+W^-$ 

Figure 4: The correlation function $R(Q)$ for like-sign particles arising from different W s for data (*closed circles*) and simulated events without Bose-Einstein symmetrization (*open circles*). The *shaded area* represents the model prediction for events with Bose-Einstein symmetrization (see text). The *solid curve* shows the result of the fit using equation (3). The *dashed and dotted curves* are results of fits to $R(Q)$ distributions for like-sign particles measured in Z^0 decays.